

# Spike-Timing-Dependent Plasticity for Bernoulli Message Passing

Sepideh Adamiat<sup>1</sup>, Wouter M. Kouw<sup>1</sup>, and Bert de Vries<sup>1,2</sup>

<sup>1</sup> Electrical Engineering Department, TU Eindhoven, Netherlands

<sup>2</sup> Lazy Dynamics B.V., Eindhoven, Netherlands

[s.adamiat@tue.nl](mailto:s.adamiat@tue.nl)

**Abstract.** Bayesian inference provides a principled framework for understanding brain function, while neural activity in the brain is inherently spike-based. This paper bridges these two perspectives by designing spiking neural networks that simulate Bayesian inference through message passing for Bernoulli messages. To train the networks, we employ spike-timing-dependent plasticity, a biologically plausible mechanism for synaptic plasticity which is based on the Hebbian rule. Our results demonstrate that the network's performance closely matches the true numerical solution. We further demonstrate the versatility of our approach by implementing a factor graph example from coding theory, illustrating signal transmission over an unreliable channel.

**Keywords:** Bayesian inference · factor graphs · message passing · leaky integrate-and-fire neurons · spiking neural networks · spike-timing-dependent plasticity.

## 1 Introduction

Numerous perceptual and motor tasks carried out by the human nervous system can be effectively described using a Bayesian inference framework [15, 7]. According to the Bayesian brain hypothesis, the brain updates its beliefs about the world by integrating sensory input with prior knowledge [4]. This concept aligns with the Free Energy Principle (FEP), which asserts that living systems adapt to their environment by maximizing evidence for an internal generative model of sensory observations [9]. This adaptation process is conceptually carried out by variational free energy minimization, physically realized by exchanging action potentials between neurons.

Recent studies have explored the information processing capacity of in vitro biological neurons cultured on top of multi-electrode arrays, demonstrating their potential for unsupervised learning, speech recognition, and decision-making tasks [3]. Some of these studies have employed the Free Energy Principle, including research by [14], which harnesses the inherent adaptive computation of neurons in a simulated game world, and [13], which investigates their application in blind source separation. These studies are evidence supporting the FEP and Bayesian Brain hypothesis.

Bayesian inference can be computationally intensive due to the complexity of integrating and marginalizing over probability distributions. Graphical representations help to manage this complexity by breaking the problem into smaller, localized computations. These graphical models provide a structured framework for inference, where message-passing algorithms (also known as belief propagation) efficiently compute posterior probabilities by passing information along the graph’s edges. This approach simplifies inference for large and sparsely connected systems, making Bayesian methods suitable for practical applications [19]. Interestingly, active inference, which is a corollary of FEP, can also be realized by message passing on a factor graph representation of the generative model [10].

On the other hand, from a biological point of view, all electrical communication in the brain is realized by spike-based message passing, and to understand the brain’s behavior or communicate with cultured neurons, we need to encode and decode information in spike forms. Spiking Neural Networks (SNNs) are a class of artificial neural networks that provide a more accurate simulation of neural processes, making them significant for advances in computational neuroscience [20]. These biologically inspired neural models communicate with each other by discrete spike trains as input and output. There are several advances in using SNNs in machine learning tasks, including [29], which implemented reinforcement learning to control an inverted pendulum problem, and [17] that proposed a self-learning spiking network to control a mobile robot. These studies highlight the potential of SNNs for robotic control and autonomous decision making. SNNs are also recognized for their efficient energy consumption when running on neuromorphic devices [30].

Numerous studies have explored the biological plausibility of message passing algorithms [25]. In [21], an innovative approach to implementing sum-product message passing within spiking neural networks is introduced. This approach utilizes a network of interconnected liquid state machines. While their work offers valuable insights into bridging the gap between SNNs and message passing, it does not address the implementation of a learning mechanism for synaptic weights—a gap that this paper aims to fill.

This paper presents a method for training SNNs with spike-timing-dependent plasticity (STDP), a biologically inspired synaptic update rule widely used in neuromorphic computing, to implement sum-product message passing for Bernoulli-distributed messages. We demonstrate that the proposed networks, constructed with a minimal number of neurons and synaptic connections, yield results closely aligned with numerical results. Furthermore, we apply the proposed network to an example of a noisy signal transmission channel, demonstrating the principles and generality of our approach.

## 2 Background

In this section, we outline two key concepts we aim to connect: Bayesian inference with message passing and spiking neural networks. Readers already familiar with these topics may choose to skip this section.

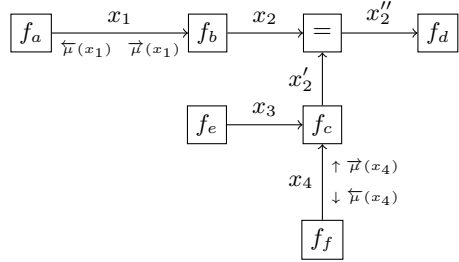


Fig. 1: The FFG corresponding to the example model defined in Equation (1).

## 2.1 Message Passing on Forney-style Factor Graphs

Sum-product message passing, or belief propagation, in Forney-style Factor Graphs (FFGs) is a powerful algorithm for performing Bayesian inference. A large variety of algorithms in fields of machine learning, signal processing, coding, and statistics may be viewed as special cases of this method [19] [18] [24]. An FFG offers a graphical description of a factorized function [8]. In an FFG, nodes represent functions, and edges represent variables. An edge connects to a node if and only if it represents a variable that is an argument of the node's function. As an example, consider the factorized function

$$f(x_1, x_2, x_3, x_4) = f_a(x_1)f_b(x_1, x_2)f_c(x_2, x_3, x_4)f_d(x_2)f_e(x_3)f_f(x_4), \quad (1)$$

with its corresponding FFG is illustrated in Figure 1. Note that in an FFG, each edge can maximally connect to two nodes. If a variable is an argument in more than two factors, we use an "equality" node  $f(x, y, z) = \delta(z - y)\delta(z - x)$  that enforces the same beliefs across all variables ( $x$ ,  $y$  and  $z$ ) that connect to the equality node.

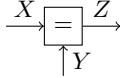
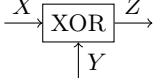
The sum-product algorithm passes "messages", which are probabilistic distributions, along the graph's edges. This method is an efficient approach for conducting probabilistic inference within sparsely connected generative models. Message-passing-based inference is particularly scalable because it exploits the model's independence structure, significantly reducing the computational complexity compared to naive Bayesian inference, which requires summing over all possible configurations globally. The local and distributed nature of the sum-product algorithm allows it to handle large-scale problems efficiently, making it widely applicable in areas such as multi-agent trajectory planning [6], control of non-linear systems [1] and active inference in non-linear environments [16].

In FFG, messages are passed bidirectionally along the edges. For notational convenience, we assign a direction to each edge and denote messages propagating in the designated direction by  $\vec{\mu}(\cdot)$ , while those traveling in the opposite direction are represented by  $\vec{\mu}(\cdot)$ . In general, for any node  $f(y, x_1, \dots, x_n)$ , the sum-product rule for an outgoing message over edge  $y$  is given by

$$\underbrace{\overrightarrow{\mu}_y(y)}_{\text{outgoing messages}} = \int \underbrace{\overrightarrow{\mu}_{x_1}(x_1) \dots \overrightarrow{\mu}_{x_n}(x_n)}_{\text{incoming messages}} \underbrace{f(y, x_1, \dots, x_n)}_{\text{node function}} dx_1 \dots dx_n. \quad (2)$$

By pre-calculating the update rules for common model components, one can efficiently construct and adjust inference algorithms without extensive computation. Certain studies have proposed message update rules [19, 28], while there exist software toolboxes that provide the pre-computed message update rules for commonly used distributions and factors [2, 22] to automate the inference process for making applications. Tables 1 present some key update rules for processing incoming messages that carry a Bernoulli distribution. In this study, we aim to implement these computations using spiking neural networks, offering a biologically inspired approach to probabilistic inference.

Table 1: Sum-product message update rules for the equality and XOR nodes, for given input messages  $\overrightarrow{\mu}_x(x) = \text{Ber}(x|p_x)$  and  $\overrightarrow{\mu}_y(y) = \text{Ber}(y|p_y)$  [18].

<i>Node function</i>	<i>Update rule</i>
	$\overrightarrow{\mu}_z(z) = \text{Ber}(z   \frac{p_x p_y}{1 - p_x + 2p_x p_y - p_y})$
	$\overrightarrow{\mu}_z(z) = \text{Ber}(z   p_x - 2p_x p_y + p_y)$

## 2.2 Spiking Neural Networks

SNNs are a class of artificial neural networks that more closely mimic biological neural systems compared to traditional artificial neural networks. Unlike standard models that use continuous activation values, SNNs process and transmit information using discrete spike events over time. This event-driven paradigm makes SNNs well-suited for combining with MP, and also enables more energy-efficient computation.

**Neuron Models** SNNs employ neuron models that describe the dynamics of membrane potential and spike generation. One of the most commonly used models is the Leaky Integrate-and-Fire (LIF) neuron, which approximates the behavior of a biological neuron with a differential equation. The membrane potential  $V(t)$  evolves according to

$$\tau_m \frac{dV(t)}{dt} = -(V(t) - V_{\text{rest}}) + RI(t),$$

where  $\tau_m$  is the membrane time constant,  $V_{\text{rest}}$  is the resting membrane potential,  $R$  is the membrane resistance,  $I(t)$  is the synaptic input current [11].  $I(t)$  represents the weighted sum of spikes from presynaptic neurons, capturing the total synaptic input to the neuron.

The leak mechanism refers to the gradual decay of the membrane potential  $V(t)$  back toward its resting value  $V_{\text{rest}}$  in the absence of input. This models the natural tendency of neurons to return to a stable baseline and prevents indefinite accumulation of input. The integrating aspect represents the accumulation of incoming currents  $I(t)$ , which drive  $V(t)$  upward. When the membrane potential reaches a certain threshold  $V_{\text{th}}$ , the neuron fires: it emits a spike (action potential), and the membrane potential is immediately reset to a lower value  $V_{\text{reset}}$ . This is the fire mechanism, mimicking the all-or-nothing nature of biological spikes. After firing, the neuron may enter a refractory period during which it is temporarily unable to spike, ensuring separation between consecutive spikes and limiting firing rates.

**Synaptic Models** Synaptic models in SNNs determine how spikes from presynaptic neurons affect the membrane potential of postsynaptic neurons. In addition to shaping input currents, synapses can also adapt over time through learning mechanisms. One biologically inspired form of synaptic plasticity is STDP, which adjusts synaptic weights based on the relative timing of pre- and postsynaptic spikes. The change in synaptic weight  $\Delta w$  is typically modeled as

$$\Delta w = \begin{cases} A_+ \exp\left(-\frac{\Delta t}{\tau_+}\right) & \text{if } \Delta t \geq 0 \\ -A_- \exp\left(\frac{\Delta t}{\tau_-}\right) & \text{if } \Delta t < 0, \end{cases}$$

where  $\Delta t = t_{\text{post}} - t_{\text{pre}}$  is the time difference between the postsynaptic and presynaptic spikes,  $A_+$  and  $A_-$  are learning rates, and  $\tau_+$  and  $\tau_-$  are time constants for potentiation and depression, respectively [26].

In summary, STDP strengthens synapses when the presynaptic neuron fires shortly before the postsynaptic neuron and weakens them when the order is reversed, thus encoding temporal correlations in spike activity.

### 3 Methodology

In this section, we introduce networks of LIF neurons trained with the biologically plausible synaptic learning rule, STDP, to simulate factor nodes in the message passing algorithm. This is achieved by encoding Bernoulli distributions into spike trains, passing them through the proposed networks, and decoding the output spike trains back into Bernoulli distributions. The output messages are compared with the numerical results derived from the sum-product

rule (2). The code used to produce the results in this paper is available at <https://github.com/biaslab/stdp-bernoulli-message-passing>.

Since this study focuses on Bernoulli messages, we start with basic logical operations AND, OR, and NOT, shown in Table 2. Functionally complete sets, such as {AND, NOT} or {OR, NOT}, serve as the foundation of logical computation, allowing for the construction of any logical operation through combinations of these primitives [5]. As a further example, we implement the XOR factor node using a combination of the AND, OR, and NOT networks. The architecture of

Table 2: Logical Gates. The logical relationships defined here specify the desired output signals for training the networks using STDP.

<b><math>S_1</math></b>	<b><math>S_2</math></b>	<b><math>OR</math></b>	<b><math>AND</math></b>	<b><math>NOT-S_1</math></b>	<b><math>XOR</math></b>
0	0	0	0	1	0
0	1	1	0	1	1
1	0	1	0	0	1
1	1	1	1	0	0

the proposed spiking neural network is illustrated in Figure 2. Each circle represents a LIF neuron. The network consists of three layers: input, output, and a temporary training layer. The input layer comprises two neurons, each receiving encoded spike trains of the input Bernoulli messages. To encode Bernoulli distributions as spike trains, we sample them at a rate of 100 samples per second (i.e., every 10 ms). These input neurons are connected to the output neuron via trainable synaptic weights, denoted as  $\omega_1$  and  $\omega_2$ , which are trained to produce the desired logical output.

To facilitate training, a training layer is used to activate the output neuron during learning; this layer is removed after training is complete. According to the STDP learning rule, synapses are strengthened when the output neuron fires shortly after the input spikes. During training, we generate the correct output spike trains based on the truth table shown in Table 2. These target spike trains are delayed by 1 ms and provided to the network via the positive training neuron, to activate the output neuron slightly after the input neurons. To weaken synapses when no spike is expected in the true output, we preemptively activate the output neuron 1 ms before the input spikes occur. This mechanism ensures that STDP decreases the synaptic strength in undesired scenarios.

Table 3: The parameter values used for LIF and STDP in section 3.

<b><math>V_{th}</math></b>	<b><math>V_{rest}</math></b>	<b><math>\tau_m</math></b>	<b><math>R</math></b>	<b><math>w_{max}</math></b>	<b><math>w_{min}</math></b>
-50 mV	-80 mV	5 ms	1	1	-1
$a^+$	$a^-$	$\tau^+$	$\tau^-$	$t_{interval}$	$lr$
0.005	$-a^+$	20 ms	20 ms	5 ms	0.005

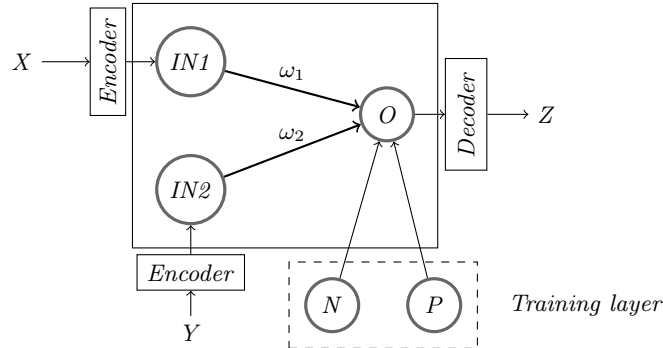


Fig. 2: SNN architecture for simulating the sum-product update rules of AND, OR, and NOT factor nodes, as represented in Table 4. Random variables  $X$  and  $Y$  are encoded into spike trains, and the resulting output spike train is decoded into  $Z$ . Each circle represents a LIF neuron. The training layer is removed after training the synaptic weights  $\omega_1$  and  $\omega_2$  using the STDP algorithm. For computing NOT of  $X$ , the variable  $Y$  is configured to emit constant spikes at every time step by defining its Bernoulli distribution as  $\overrightarrow{\mu}_y(y) = \text{Ber}(y | p_y = 1)$ .

The evolution of the synaptic weights  $\omega_1$  and  $\omega_2$  during training is shown in Figure 4. This training approach is inspired by [23], and all neuron and synapse model parameters follow that study. The parameter values are summarized in Table 3. We used the Brian2 toolbox [12] to simulate neural activities.

For training, the input probabilities  $p_x$  and  $p_2$  are initially set to 0.5. However, for the NOT operation, where the goal is to compute the negation of input 1, we fix  $p_y = 1$ , ensuring that the second input neuron fires at every time step. As shown in the figure, the network learns to strengthen the synaptic connection  $\omega_2$  while weakening  $\omega_1$ . This effectively causes the output neuron to spike only when input 1 does not spike, correctly implementing the NOT function.

After the training phase, the training layer is removed, and the spikes from the output neuron are decoded into a Bernoulli distribution. The output message is defined as

$$\overrightarrow{\mu}_z(z) = \text{Ber}(z | p_z), \quad p_z = \rho/\tau \quad (3)$$

where  $\rho$  represents the total spike count observed at the output neuron, and  $\tau$  is defined as the total number of samples drawn from the input messages. In this decoding process,  $\mu_z(z)$  reflects the probability that the output neuron fires.

Figure 3 compares these decoded results with the numerical outcomes obtained from the sum-product update rule defined in (2), as summarized in Table 4. The derivation details are provided in Appendix A. As shown in Figure 3, the proposed spiking-based method closely matches the numerical results.

The proposed networks can be used to implement more complex logical operations. As an example, we construct the XOR operation using combinations of the basic logical networks; its architecture is shown in Figure 5. In Figure 3, the

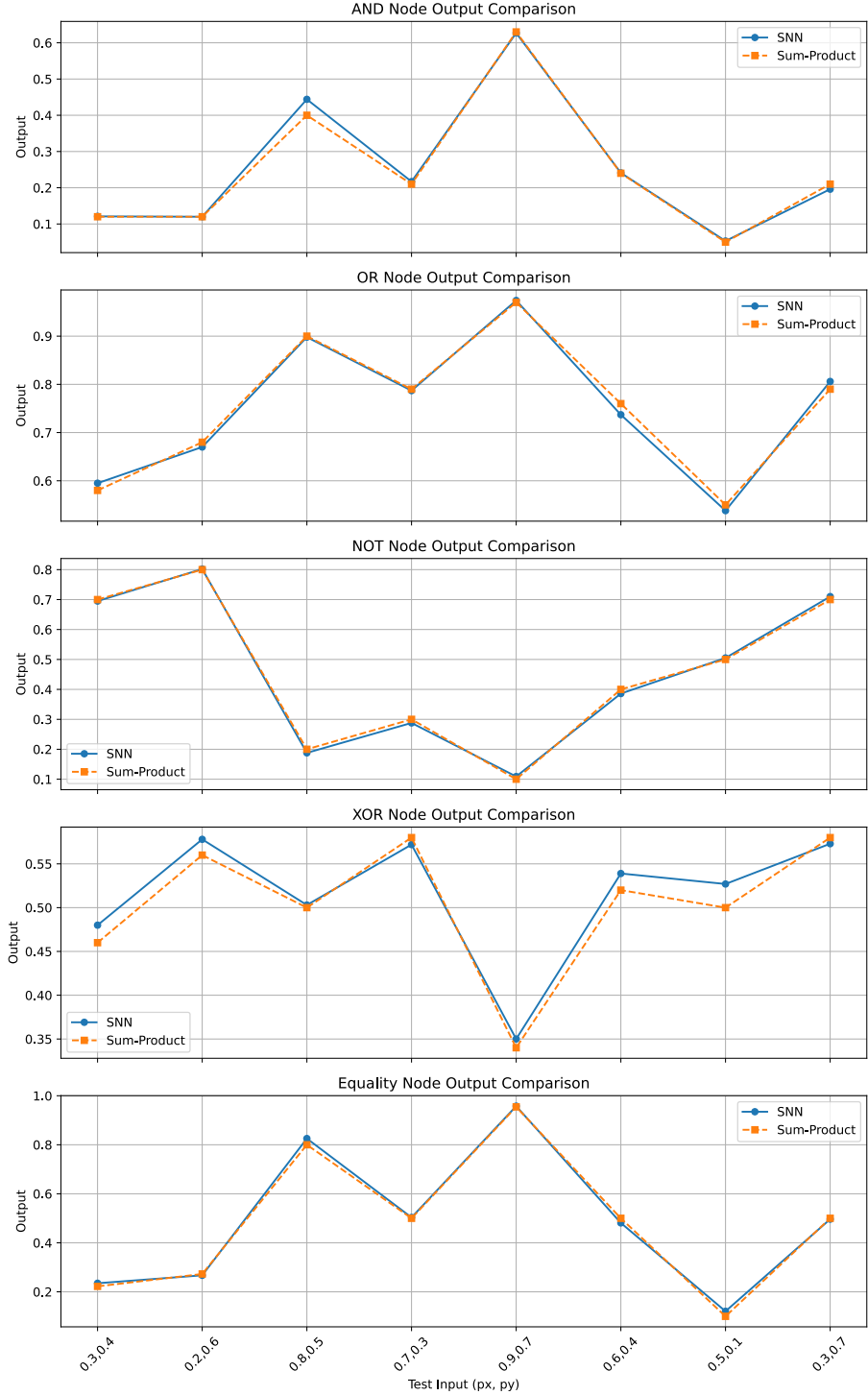


Fig. 3: Comparison of the results obtained from the proposed SNN-based nodes for passing Bernoulli messages with those produced by the sum-product algorithm. Validation was performed using eight random pairs of  $p_x$  and  $p_y$ .

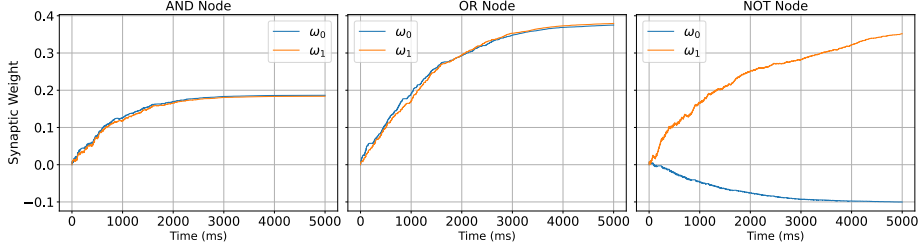


Fig. 4: Evolution of synaptic weights for AND, OR, and NOT nodes, from STDP-based training described in Section 3.

Table 4: Sum-product message update rules for the AND, OR, and NOT nodes, for given input messages  $\vec{\mu}_x(x) = \text{Ber}(x|p_x)$  and  $\vec{\mu}_y(y) = \text{Ber}(y|p_y)$ . Detailed derivations are provided in Appendix A.

Node function	Update rule
$\begin{array}{c} X \xrightarrow{\text{AND}} Z \\ \uparrow Y \end{array}$	$\vec{\mu}_z(z) = \text{Ber}(z p_x p_y)$
$\begin{array}{c} X \xrightarrow{\text{OR}} Z \\ \uparrow Y \end{array}$	$\vec{\mu}_z(z) = \text{Ber}(z p_x - p_x p_y + p_y)$
$\begin{array}{c} X \xrightarrow{\text{NOT}} Z \end{array}$	$\vec{\mu}_z(z) = \text{Ber}(z 1 - p_x)$

output of the spiking-based XOR implementation is compared with the numerical results obtained from the sum-product update rule, as presented in Table 1.

The final operation we address in this paper is the equality constraint, a fundamental factor node in the sum-product algorithm. Although it is not a logical operation in the traditional sense, it can still be simulated using the proposed spiking networks. We expect a behavior consistent with the values reported in Table 5 for the equality constraint. As shown in the table, the total number of output spikes, denoted by  $\rho$  in (3), closely resembles the result of an AND operation applied to the input spike trains. To determine an appropriate value for  $\tau$  in (3) under this constraint, cases labeled as 'Not Defined' are excluded from the to-

Table 5: Equality Constraint. The table presents the expected output spike behavior of an equality node.

$S_1$	$S_2$	Equality
0	0	0
0	1	Not Defined
1	0	Not Defined
1	1	1

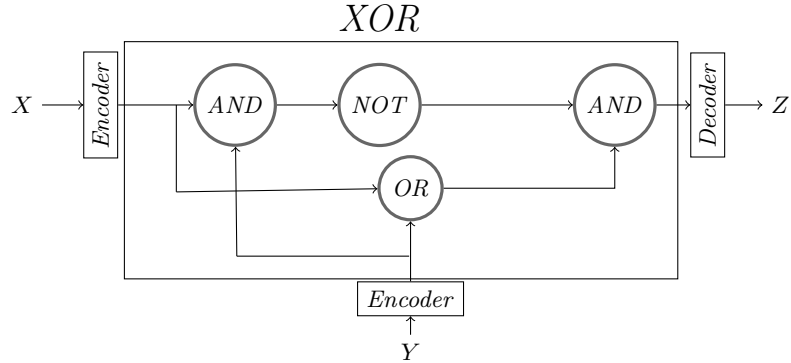


Fig. 5: SNN architecture for simulating the sum-product update rule of XOR factor node as defined in Table 1. The component networks reused from the AND, OR, and NOT implementations are shown in Figure 2, and the same encoding and decoding methods are applied.

tal number of samples. Interestingly, these cases align with the spike count of the XOR logical operation. The final outcome is compared in Figure 3 with the numerical sum-product result, obtained using the update rules presented in Table 1.

#### 4 Example

In this section, we evaluate the inference capability of the proposed spiking network model using an example based on an unreliable binary communication channel. This signal transmission scenario has been used in prior work [18] [27] as a benchmark for evaluating Bernoulli message-passing algorithms. Consider a simple binary code  $C = \{(0, 0, 0, 0), (0, 1, 1, 1), (1, 0, 1, 1), (1, 1, 0, 0)\}$  illustrated as a FFG in Figure 6 (left). Each bit of a binary codeword  $X = (x_1, x_2, x_3, x_4)$  is transmitted through an unreliable communication channel with a known bit-flip (cross-over) probability of  $\varepsilon = 0.1$ . The generative model is given by

$$f(x_1, \dots, x_4, z | y_1, \dots, y_4) \propto f_{xor}(x_1, x_2, z) f_{=(x_3, x_4, z)} \prod_{i=1}^4 p(y_i | x_i).$$

where  $z$  is a latent variable and the  $y_i$  are noisy observations. Given the observed values  $(y_1, y_2, y_3, y_4) = (0, 0, 1, 0)$ , the corresponding Bernoulli messages can be obtain as

$$(\vec{\mu}_{x_1}(x_1), \vec{\mu}_{x_2}(x_2), \vec{\mu}_{x_3}(x_3), \vec{\mu}_{x_4}(x_4)) = (\text{Ber}(0.1), \text{Ber}(0.1), \text{Ber}(0.9), \text{Ber}(0.1)).$$

as detailed in Appendix B.

The goal is to compute the marginal posterior for each bit  $x_i$ . The table in Figure 6 (right) compares all the messages produced by our SNN-based model

with the ground-truth messages passed along each edge of the FFG. The results show that our method closely approximates the expected message values. Finally, the marginal posteriors are obtained via the normalized product

$$\overrightarrow{\mu}_{x_i}(x_i) \times \overleftarrow{\mu}_{x_i}(x_i) = \text{Ber}(0.109), \text{Ber}(0.109), \text{Ber}(0.168), \text{Ber}(0.175), \quad (4)$$

which closely match the messages produced by the sum-product rule  $\text{Ber}(0.1)$ ,  $\text{Ber}(0.1)$ ,  $\text{Ber}(0.18)$ ,  $\text{Ber}(0.18)$  [18].

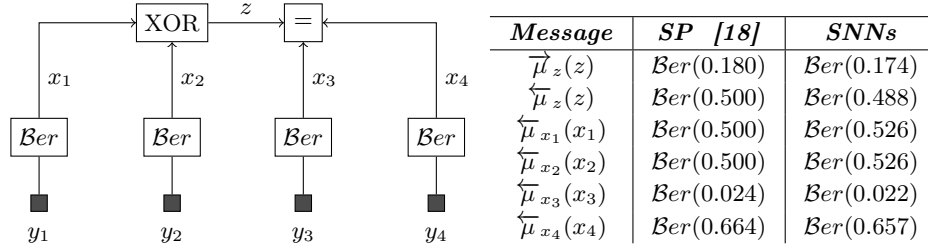


Fig. 6: (Left) The FFG corresponding to the unreliable binary channel example. (Right) The sum-product calculated messages versus messages produced by the SNNs.

## 5 Conclusions

We presented a biologically plausible network of spiking neurons trained using STDP to perform message-passing for Bernoulli messages. This work represents a potential step toward bridging the gap between theoretical models of brain function, such as the Bayesian Brain hypothesis and the FEP, and the spiking behavior of biological neurons.

**Acknowledgments.** This work was carried out in the context of the BayesBrain project. We gratefully acknowledge financial support from the Eindhoven Artificial Intelligence Systems Institute (EAISI) at TU Eindhoven.

**Disclosure of Interests.** The authors declare no conflict of interest.

## A Derivation of Sum-Product Update Rules

We can derive the forward sum-product message  $\overrightarrow{\mu}_z(z)$  according to (2), given the input messages  $\overrightarrow{\mu}_x(x) = \text{Ber}(x|p_x)$  and  $\overrightarrow{\mu}_y(y) = \text{Ber}(y|p_y)$ .

$$\begin{aligned}\overrightarrow{\mu}_z(z) &= \sum_x \sum_y \overrightarrow{\mu}_x(x) \overrightarrow{\mu}_y(y) f(z, x, y) \\ &= \text{Ber}(0|p_x) \text{Ber}(0|p_y) f(z, 0, 0) + \text{Ber}(1|p_x) \text{Ber}(0|p_y) f(z, 1, 0) \\ &\quad + \text{Ber}(0|p_x) \text{Ber}(1|p_y) f(z, 0, 1) + \text{Ber}(1|p_x) \text{Ber}(1|p_y) f(z, 1, 1) \\ &= (1 - p_x)(1 - p_y) f(z, 0, 0) + p_x(1 - p_y) f(z, 1, 0) \\ &\quad + (1 - p_x)p_y f(z, 0, 1) + p_x p_y f(z, 1, 1).\end{aligned}$$

Using the truth table, we can substitute  $z$  and evaluate the terms for different operations. As an example, the AND operation is

$$\begin{aligned}\overrightarrow{\mu}_z(z) &= \begin{cases} p_x p_y & \text{if } z = 1 \\ (1 - p_x)(1 - p_y) + p_x(1 - p_y) + (1 - p_x)p_y & \text{if } z = 0 \end{cases} \\ &= \begin{cases} p_x p_y & \text{if } z = 1 \\ 1 - p_x p_y & \text{if } z = 0 \end{cases} = \text{Ber}(z|p_x p_y).\end{aligned}$$

Similarly, we have the following computations for the OR factor node

$$\begin{aligned}\overrightarrow{\mu}_z(z) &= \begin{cases} p_x p_y + p_x(1 - p_y) + (1 - p_x)p_y & \text{if } z = 1 \\ (1 - p_x)(1 - p_y) & \text{if } z = 0 \end{cases} \\ &= \begin{cases} p_x + p_y - p_x p_y & \text{if } z = 1 \\ 1 - p_x - p_y + p_x p_y & \text{if } z = 0 \end{cases} = \text{Ber}(z|p_x + p_y - p_x p_y).\end{aligned}$$

## B Derivation of Messages in the Example

Under the bit-flip channel model, the likelihood is given by

$$p(y_i|x_i) = \begin{cases} (1 - \varepsilon)x_i + \varepsilon(1 - x_i) & \text{if } y_i = 1 \\ \varepsilon x_i + (1 - \varepsilon)(1 - x_i) & \text{if } y_i = 0 \end{cases} = \text{Ber}(y_i|(1 - \varepsilon)x_i + \varepsilon(1 - x_i)).$$

According to the sum-product rule, the messages can be obtained by

$$\begin{aligned}\overrightarrow{\mu}_{x_i}(x_i) &= \sum_{y_i \in \{0, 1\}} \delta(y_i - \hat{y}_i) \text{Ber}(y_i|(1 - \varepsilon)x_i + \varepsilon(1 - x_i)) \\ &= \begin{cases} (1 - \varepsilon)x_i + \varepsilon(1 - x_i) & \text{if } \hat{y}_i = 1 \\ \varepsilon x_i + (1 - \varepsilon)(1 - x_i) & \text{if } \hat{y}_i = 0 \end{cases} \\ &= \begin{cases} \text{Ber}(x_i|1 - \varepsilon) & \text{if } \hat{y}_i = 1 \\ \text{Ber}(x_i|\varepsilon) & \text{if } \hat{y}_i = 0 \end{cases}.\end{aligned}$$

## References

1. Adamiat, S., Kouw, W.M., van Erp, B., de Vries, A.B.: Message passing-based Bayesian control of a cart-pole system. In: International Workshop on Active Inference. Springer (2024)
2. Bagaev, D., de Vries, B.: Reactive message passing for scalable bayesian inference. *Scientific Programming* **2023**(1), 6601690 (2023)
3. Cai, H., Ao, Z., Tian, C., Wu, Z., Liu, H., Tchieu, J., Gu, M., Mackie, K., Guo, F.: Brain organoid reservoir computing for artificial intelligence. *Nature Electronics* **6**(12), 1032–1039 (2023)
4. Doya, K.: Bayesian brain: Probabilistic approaches to neural coding. MIT Press (2007)
5. Enderton, H.B.: A mathematical introduction to logic. Elsevier (2001)
6. van Erp, B., Bagaev, D., Podusenko, A., İsmail, S., de Vries Bert: Multi-agent trajectory planning with NUV priors. American Control Conference (2024, in press)
7. Fiorillo, C.D., Tobler, P.N., Schultz, W.: Discrete coding of reward probability and uncertainty by dopamine neurons. *Science* **299**(5614), 1898–1902 (2003)
8. Forney, G.D.: Codes on graphs: Normal realizations. *IEEE Transactions on Information Theory* **47**(2), 520–548 (2001)
9. Friston, K., Kilner, J., Harrison, L.: A free energy principle for the brain. *Journal of Physiology* **100**(1-3), 70–87 (2006)
10. Friston, K.J., Parr, T., de Vries, B.: The graphical brain: Belief propagation and active inference. *Network Neuroscience* **1**(4), 381–414 (2017)
11. Gerstner, W., Kistler, W.M.: Spiking neuron models: Single neurons, populations, plasticity. Cambridge University Press (2002)
12. Goodman, D.F., Brette, R.: Brian: a simulator for spiking neural networks in Python. *Frontiers in Neuroinformatics* **2**, 350 (2008)
13. Isomura, T., Kotani, K., Jimbo, Y.: Cultured cortical neurons can perform blind source separation according to the free-energy principle. *PLoS Computational Biology* **11**(12), e1004643 (2015)
14. Kagan, B.J., Kitchen, A.C., Tran, N.T., Habibollahi, F., Khajehnejad, M., Parker, B.J., Bhat, A., Rollo, B., Razi, A., Friston, K.J.: In vitro neurons learn and exhibit sentience when embodied in a simulated game-world. *Neuron* **110**(23), 3952–3969 (2022)
15. Knill, D.C., Richards, W.: Perception as Bayesian inference. Cambridge University Press (1996)
16. Van de Laar, T.W., De Vries, B.: Simulating active inference processes by message passing. *Frontiers in Robotics and AI* **6**, 20 (2019)
17. Lobov, S.A., Mikhaylov, A.N., Shamshin, M., Makarov, V.A., Kazantsev, V.B.: Spatial properties of STDP in a self-learning spiking neural network enable controlling a mobile robot. *Frontiers in Neuroscience* **14**, 88 (2020)
18. Loeliger, H.A.: An introduction to factor graphs. *IEEE Signal Processing Magazine* **21**(1), 28–41 (2004)
19. Loeliger, H.A., Dauwels, J., Hu, J., Krol, S., Ping, L., Kschischang, F.R.: The factor graph approach to model-based signal processing. *Proceedings of the IEEE* **95**(6), 1295–1322 (2007)
20. Maass, W.: Networks of spiking neurons: the third generation of neural network models. *Neural Networks* **10**(9), 1659–1671 (1997)
21. Maass, W.: Liquid state machines: motivation, theory, and applications. *Computability in Context* pp. 275–296 (2011)

22. Minka, T., Winn, J., Guiver, J., Zaykov, Y., Fabian, D., Bronskill, J.: /Infer.NET 0.3 (2018), microsoft Research Cambridge. <http://dotnet.github.io/infer>
23. Mo, L., Wang, M.: Logicsnn: A unified spiking neural networks logical operation paradigm. *Electronics* **10**(17), 2123 (2021)
24. Palmieri, F.A., Pattipati, K.R., Di Gennaro, G., Fioretti, G., Verolla, F., Buananno, A.: A unifying view of estimation and control using belief propagation with application to path planning. *IEEE Access* **10**, 15193–15216 (2022)
25. Parr, T., Markovic, D., Kiebel, S.J., Friston, K.J.: Neuronal message passing using mean-field, bethe, and marginal approximations. *Scientific reports* **9**(1), 1889 (2019)
26. Song, S., Miller, K.D., Abbott, L.F.: Competitive hebbian learning through spike-timing-dependent synaptic plasticity. *Nature neuroscience* **3**(9), 919–926 (2000)
27. Steimer, A., Maass, W., Douglas, R.: Belief propagation in networks of spiking neurons. *Neural Computation* **21**(9), 2502–2523 (2009)
28. Winn, J., Bishop, C.M., Jaakkola, T.: Variational message passing. *Journal of Machine Learning Research* **6**(4) (2005)
29. Wu, G., Liang, D., Luan, S., Wang, J.: Training spiking neural networks for reinforcement learning tasks with temporal coding method. *Frontiers in Neuroscience* **16**, 877701 (2022)
30. Yamazaki, K., Vo-Ho, V.K., Bulsara, D., Le, N.: Spiking neural networks and their applications: A review. *Brain sciences* **12**(7), 863 (2022)